International Journal of Thermophysics, Vol. 20, No. 3, 1999

Bubble-Point Pressures and Saturated- and Compressed-Liquid Densities of the Binary R-125 + R-143a System[1]

T. Fujimine,[2,3] H. Sato,[2] and K. Watanabe[2]

Bubble-point pressures and saturated- and compressed-liquid densities of the binary R-125 (pentafluoroethane) + R-143a (1,1,1-trifluoroethane) system have been measured for several compositions at temperatures from 280 to 330 K by means of a magnetic densimeter coupled with a variable-volume cell mounted with a metallic bellows. The experimental uncertainties of the temperature, pressure, density, and composition were estimated to be within ±10 mK, ±12 kPa, ±0.2%, and ±0.2 mass%, respectively. The purities of the samples used throughout the measurements are 99.96 area% for R-125 and 99.94 area% for R-143a. Based on these measurements, the thermodynamic behavior of the vapor–liquid equilibria of this binary refrigerant mixture has been represented using the Peng–Robinson equation for the bubble-point pressures, a correlation for the saturated-liquid densities, and an equation of state for the compressed-liquid densities.

KEY WORDS: alternative refrigerant; binary R-125 + R-143a mixtures; bubble-point pressure; compressed-liquid density; R-125; R-143a; saturated-liquid density; vapor–liquid equilibria.

1. INTRODUCTION

Recent concerns about the environmental effects of CFC and HCFC alternatives have caused HFC refrigerant mixtures to be considered as prospective replacements for some CFCs and HCFCs. The nonflammable R-125 and the flammable R-143a both have vapor pressures similar to those of

[1] Paper presented at the Thirteenth Symposium on Thermophysical Properties, June 22–27, 1997, Boulder, Colorado, U.S.A.

[2] Department of System Design Engineering, Faculty of Science and Technology, Keio University, 3-14-1 Hiyoshi, Kohoku-ku, Yokohama 223-8522, Japan.

[3] To whom correspondence should be addressed.

0195-928X/99/0500-0911$16.00/0

R-502 (the azeotropic mixture of R-22 and R-115). Therefore, their mixture can be expected to be a promising alternative to replace R-502. The present work investigates the bubble-point pressures and the saturated- and compressed-liquid densities of the binary R-125 + R-143a system.

2. MEASUREMENTS AND RESULTS

All measurements in the present work were performed with a magnetic densimeter coupled with a variable volume cell which enables measurements either at the saturated-liquid condition or in the compressed liquid. The apparatus, shown schematically in Fig. 1, has been used to perform similar measurements for other alternative refrigerant mixtures [1–3]. The pressure was measured with a digital quartz pressure gauge (F, J). The sample density was directly measured by a magnetic densimeter (A), while the temperature was measured by means of a standard platinum resistance

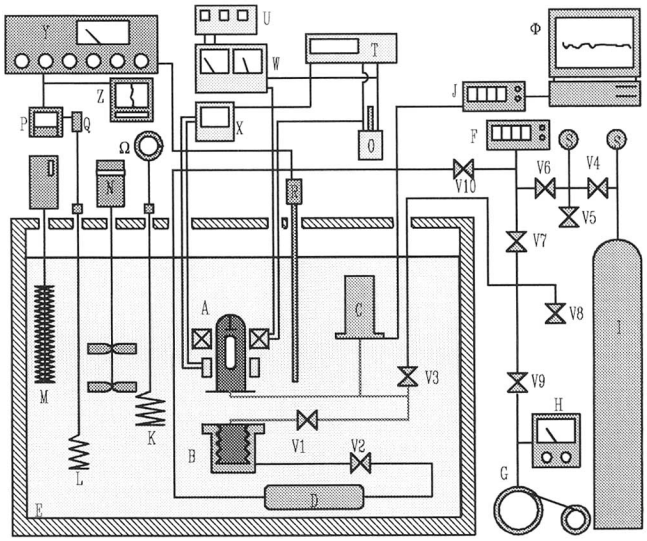

Fig. 1. Experimental apparatus. (A) Magnetic densimeter, (B) variable volume cell, (C) digital quartz pressure transducer, (D) damper, (E) thermostat, (F) digital quartz pressure gauge, (G) vacuum pump, (H) vacuum gauge, (I) nitrogen gas, (J) digital quartz pressure computer, (K) main heater, (L) subheater, (M) cooler, (N) stirrer, (O) standard resistor, (P) PID controller, (R) standard platinum resistance thermometer, (S) pressure gauge, (T) digital multimeter, (U) current controller, (V1–V10) valves, (W) DC power supply, (X) galvanometer, (Y) thermometer bridge, (Z) pen recorder, (Ω) transformer, and (Φ) personal computer.

thermometer (R) placed in the vicinity of the magnetic densimeter. Controlling the pressure of the nitrogen gas in the outer part of the metallic bellows allows the sample to be brought into the saturated- and/or compressed-liquid state. The saturation state of the mixture with known composition was determined by observing the appearance and disappearance of

Table I. Measured Bubble-Point Pressures and Saturated-Liquid Densities

T (K)	P (MPa)	ρ (kg·m^{-3})	T (K)	P (MPa)	ρ (kg·m^{-3})
		0 mol%, 0 mass% R-125			
249.981	0.281	1097.3	299.986	1.326	919.9
259.984	0.401	1065.4	299.988	1.324	918.9
269.987	0.562	1032.7	309.985	1.702	873.5
279.988	0.764	998.4	309.986	1.700	872.8
279.988	0.762	996.9	319.986	2.149	817.7
289.988	1.015	959.4	319.986	2.150	818.6
289.988	1.017	961.3	329.986	2.689	750.0
		14.61 mol%, 19.64 mass% R-125			
279.988	0.764	1047.0	309.986	1.708	916.5
289.988	1.018	1008.3	319.986	2.165	859.5
299.987	1.330	964.8			
		31.81 mol%, 39.98 mass% R-125			
279.987	0.765	1098.7	309.986	1.720	962.5
289.987	1.022	1058.6	319.986	2.180	902.5
299.986	1.337	1013.3	329.998	2.732	825.8
		41.10 mol%, 49.91 mass% R-125			
279.987	0.768	1125.6	309.986	1.729	985.8
289.987	1.028	1084.4	319.986	2.195	924.1
299.986	1.345	1037.8	329.998	2.749	844.4
		51.63 mol%, 60.39 mass% R-125			
279.987	0.773	1158.6	309.986	1.746	1012.9
289.987	1.035	1115.3	319.986	2.215	948.2
299.986	1.356	1067.0	329.998	2.776	863.9
		73.69 mol%, 80.00 mass% R-125			
279.987	0.799	1215.4	299.986	1.394	1117.9
289.987	1.067	1169.8	309.986	1.794	1058.9
		100 mol%, 100 mass% R-125			
279.988	0.827	1287.0	309.986	1.858	1112.4
289.988	1.101	1236.4	319.963	2.358	1032.3
299.987	1.443	1179.2			

Table II. Measured Compressed-Liquid $P\rho Tx$ Properties

T (K)	P (MPa)	ρ (kg·m^{-3})	T (K)	P (MPa)	ρ (kg·m^{-3})
		0 mol%, 0 mass%R-125			
249.981	0.504	1097.9	279.987	2.202	1007.8
249.981	1.001	1099.9	279.988	2.503	1009.7
249.981	1.500	1101.3	279.988	3.007	1013.7
249.981	1.993	1103.0	289.988	1.218	962.9
249.981	2.529	1104.6	289.988	1.501	965.2
249.981	3.006	1106.1	289.989	1.804	967.7
259.984	1.015	1068.4	289.987	2.203	970.8
259.984	1.538	1070.4	289.988	2.603	973.7
259.984	2.014	1072.2	289.987	3.003	976.8
259.984	2.513	1074.1	299.987	1.506	922.1
259.984	3.021	1076.2	299.986	2.002	927.4
269.987	1.031	1035.7	299.987	2.500	932.6
269.987	1.532	1038.0	299.986	3.003	937.2
269.987	2.055	1040.7	309.987	2.003	878.1
269.987	2.524	1043.0	309.986	2.505	885.5
269.987	3.013	1045.2	309.987	3.002	891.8
279.988	1.003	1000.1	319.984	2.510	827.6
279.988	1.303	1002.6	319.985	2.998	837.9
279.988	1.602	1004.3	329.985	3.013	764.0
279.988	1.901	1006.1			
		14.61 mol%, 19.64 mass% R-125			
279.988	1.008	1048.8	299.987	2.022	972.6
279.988	1.521	1052.4	299.987	2.520	978.0
279.988	2.067	1056.0	299.987	3.024	983.1
279.988	2.507	1058.9	309.986	2.140	923.6
279.988	3.013	1061.8	309.986	2.507	928.8
289.988	1.564	1013.0	309.986	3.012	936.0
289.988	2.013	1016.8	319.986	2.698	872.4
289.988	2.508	1020.8	319.986	3.013	879.4
289.988	3.027	1024.9			
		31.81 mol%, 39.98 mass% R-125			
279.988	1.076	1100.9	299.987	2.012	1021.5
279.988	1.534	1104.3	299.987	2.505	1027.0
279.988	2.015	1107.7	299.987	3.041	1032.8
279.988	2.533	1111.4	309.986	2.121	969.5
279.988	3.012	1114.6	309.986	2.526	976.1
289.988	1.611	1064.1	309.986	3.043	983.9
289.988	2.009	1067.7	319.986	2.579	913.3
289.988	2.511	1072.0	319.986	3.025	923.8
289.988	3.005	1076.0	329.985	3.033	841.7
299.987	1.526	1015.6			

Table II. *(Continued)*

T (K)	P (MPa)	ρ (kg·m^{-3})	T (K)	P (MPa)	ρ (kg·m^{-3})
		41.10 mol%, 49.91 mass% R-125			
279.988	1.090	1128.5	299.987	2.159	1047.9
279.988	1.512	1131.5	299.987	2.510	1052.1
279.988	2.012	1135.1	299.987	3.011	1057.7
279.988	2.537	1138.8	309.986	2.086	992.3
279.988	3.012	1142.0	309.986	2.522	999.6
289.988	1.542	1089.2	309.986	3.003	1007.2
289.988	2.016	1093.1	319.986	2.773	939.8
289.988	2.508	1097.0	329.985	3.008	859.0
289.988	3.011	1102.4			
		51.63 mol%, 60.39 mass% R-125			
279.988	1.029	1160.2	299.987	2.057	1076.0
279.988	1.554	1164.4	299.987	2.549	1082.0
279.988	2.043	1168.1	299.987	3.005	1087.3
279.988	2.560	1171.6	309.986	2.103	1019.5
279.988	3.040	1175.0	309.986	2.510	1026.6
289.988	1.578	1120.3	309.986	3.012	1034.8
289.988	2.003	1124.6	319.986	2.564	958.7
289.988	2.533	1129.6	319.986	3.010	970.5
289.988	3.004	1133.5	329.985	3.052	880.7
299.987	1.567	1069.7			
		73.69 mol%, 80.00 mass% R-125			
279.988	1.068	1217.2	299.987	2.027	1126.7
279.988	1.523	1221.4	299.987	2.521	1133.1
279.988	2.056	1226.0	299.987	2.998	1139.3
279.988	2.569	1229.7	309.986	2.058	1064.4
279.988	3.045	1233.1	309.986	2.545	1073.6
289.988	1.520	1174.4	309.986	2.957	1081.1
289.988	2.042	1179.5	319.986	2.618	1000.3
289.988	2.502	1184.2	319.986	3.059	1013.1
289.988	3.016	1189.1			
		100 mol%, 100 mass% R-125			
279.988	1.526	1293.5	289.988	3.025	1257.1
279.988	2.020	1297.7	299.987	2.023	1188.0
279.988	2.519	1301.6	299.987	2.528	1195.7
279.988	3.004	1306.1	299.987	3.039	1202.5
289.988	1.522	1242.0	309.986	2.531	1128.7
289.988	2.011	1246.7	309.986	3.027	1138.5
289.988	2.511	1252.2	319.963	3.012	1056.2

a bubble in the liquid phase. The sample purities, as analyzed by the chemical manufacturers, are 99.96 area% for R-125 and 99.94 area% for R-143a, respectively, and no further purification was performed. We estimated uncertainties of the measurements following the ISO guide [4] on the basis of expanded uncertainty with a coverage factor $k = 2$. The experimental uncertainties of the temperature, bubble-point pressure, density, and composition were estimated to be no greater than ± 10 mK, ± 12 kPa, $\pm 0.2\%$, and ± 0.2 mass%, respectively. The uncertainty in pressure measurements for the $P\rho Tx$ properties of the compressed liquid was estimated to be ± 2 kPa, whereas the uncertainty in bubble-point pressure measurements is ± 12 kPa due to possible error in the saturation point determination.

We have measured the bubble-point pressures and saturated- and compressed-liquid densities of the binary R-125 + R-143a system for temperatures from 280 to 330 K at 10 K intervals up to 3 MPa and for compositions of 0, 19.64, 39.98, 49.91, 60.39, 80.00, and 100 mass% R-125. We have prepared the sample mixtures by weighing the mass of each component independently and blending them to the compositions given above. The experimental results are summarized in Tables I and II.

3. DISCUSSION

The Peng–Robinson (PR) equation has been applied to represent bubble-point pressures obtained in the present work. The binary interaction parameter, k_{ij}, in this equation has been optimized and found to be $k_{ij} = -0.0126$ on the basis of the present data and the data by Nagel and Bier [5]. The critical parameters of R-125 and R-143a used throughout the present study are given in Table III. The critical temperature, density, and pressure of the binary mixtures of the present study are those determined by Higashi [6]. The relative deviation of bubble-point pressures from the PR equation at various mole fractions x_{125} of R-125 is plotted in Fig. 2. As

Table III. Critical Parameters [6]

	R-125	R-143a
T_c (K)	339.17	345.88
P_c (MPa)	3.620	3.764
ρ_c (kg · m^{-3})	577.0	431.04
M (g · mol^{-1})	120.02	84.04
ω	0.305	0.263
V^* (cm^3 · mol^{-1})	208.01	194.99

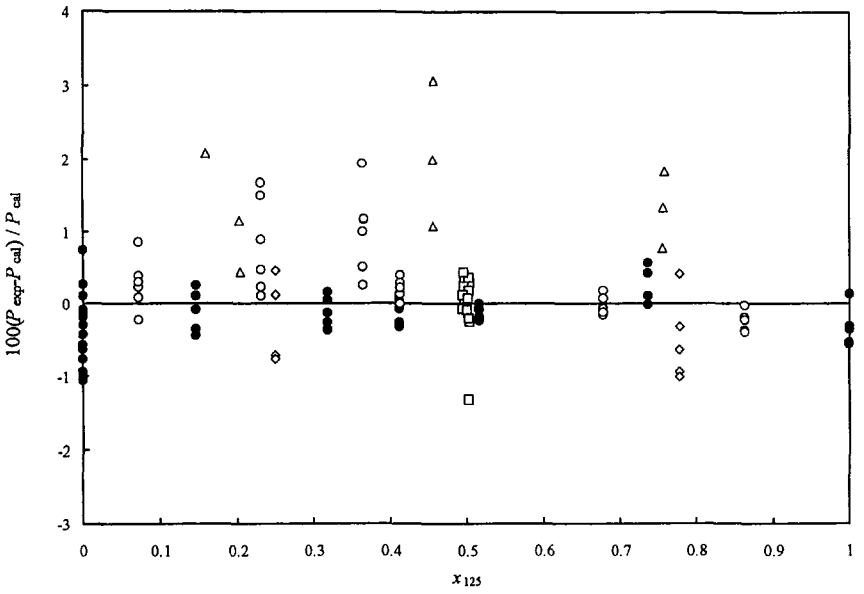

Fig. 2. Relative deviations of bubble-point pressures at different compositions from the PR equation. □ Nagel and Bier [5]; △, Takashima and Higashi [11]; ○, Widiatmo et al. [7]; ◇, Zhelezny et al. [12]; ●, this work.

shown in Fig. 2, the optimized PR equation can reproduce the present data within $\pm 1\%$, and most of the reported data agree with the PR equation within $\pm 2\%$. The effective range of the optimized PR equation covers temperatures from 200 to 330 K.

The PR equation, which is widely employed in industrial applications, is confirmed effective only in representing bubble-point pressures, and not saturated-liquid densities [7]. We applied the new correlation proposed by Widiatmo et al. [8] for the saturated-liquid densities of mixtures. The correlation is given by Eq. (1).

$$\rho_r = 1 + A_m \tau^{a_m} + B_m \tau^{b_m} + C_m \tau^{c_m} \tag{1}$$

where $\rho_r = \rho/\rho_{cm}$ and $\tau = 1 - T/T_{cm}$.

The subscript m denotes mixtures. The loci of the critical temperature, T_{cm}, the critical pressure, P_{cm}, and the critical density, ρ_{cm}, for the binary R-125 + R-143a system are those determined by Higashi [6] based on his measurements. The coefficients A_m, B_m, C_m and exponents a_m, b_m, c_m are calculated with the mixing rule, given by Eq. (2).

Table IV. Numerical Constants in Eq. (2)

	A_m	B_m	C_m	a_m	b_m	c_m
Y_1	0.42700	2.0425	0.57108	3.7043	0.35314	0.85832
Y_2	0.44411	1.7481	0.57467	0.99672	0.42913	0.26212
Y_{12}	−0.027569	−0.35070	−0.029462	−0.91893	−0.093061	−0.45603

$$Y_m = \theta_1 Y_1 + (1-\theta_1)\, Y_2 + \theta_1(1-\theta_1)\, Y_{12} \qquad (Y = A, B, C, a, b, c) \tag{2}$$

$$\theta_i = \frac{x_i V_{ci}^{2/3}}{\sum_j x_j V_{cj}^{2/3}} \tag{3}$$

θ_1 denotes the surface fraction of R-125 defined by Eq. (3). We determined the parameters used in Eq. (2) based on our data, those of Widiatmo et al. [7], and those of Ikeda and Higashi [9]. The numerical values of Y_{12} for the binary R-125 + R-143a system as well as the values of Y_1, Y_2 for pure substances, R-125 and R-143a, are given in Table IV. Figures 3 and 4 show the deviations of measured saturated-liquid densities

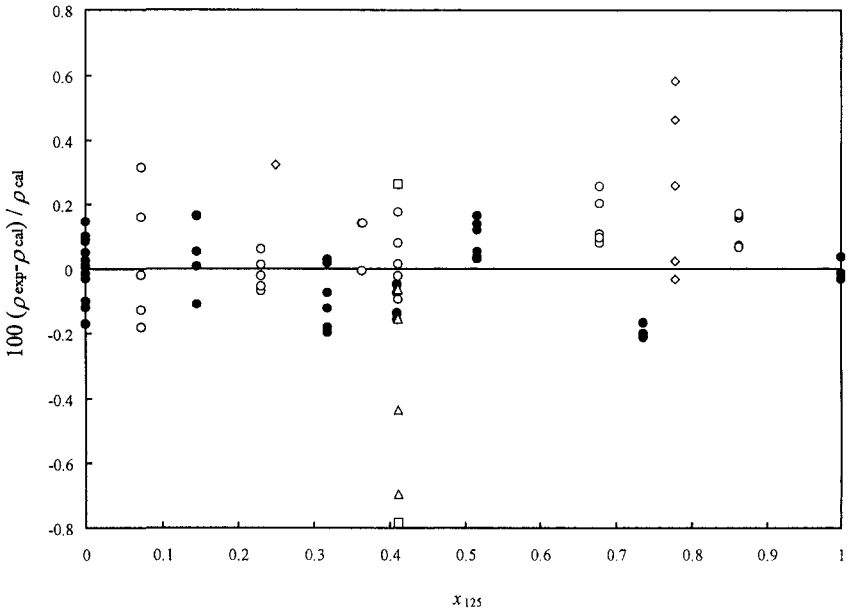

Fig. 3. Relative deviations of saturated-liquid densities at different compositions from Eq. (1). □, Kishizawa et al. [13]; △, Ikeda and Higashi [9]; ○, Widiatmo et al. [7]; ◇, Zhelezny et al. [12]; ●, this work.

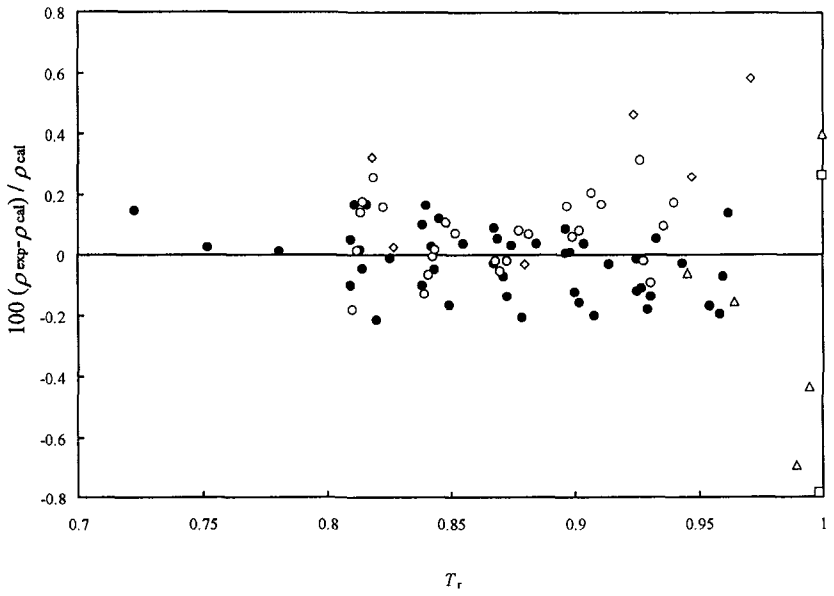

Fig. 4. Relative deviations of saturated-liquid densities at different temperatures from Eq. (1). □, Kishizawa et al. [13]; △, Ikeda and Higashi [9]; ○, Widiatmo et al. [7]; ◇, Zhelezny et al. [12]; ●, this work.

from Eq. (1), which represents the present data within ±0.2%. Since most of the reported data agree with Eq. (1) within ±0.3%, Eq. (1) seems to be an appropriate saturated-liquid density representation for the binary R-125 + R-143a system. The effective range of Eq. (1) covers temperatures from 280 to 330 K.

Sato [10] proposed an empirical equation to represent the liquid-phase $P\rho T$ properties of water, which is given as follows:

$$\rho_r = (P_r + E)^D / F \tag{4}$$

We have applied this model for representing the present compressed-liquid $P\rho Tx$ properties and saturated-liquid densities of the binary R-125 + R-143a system as follows:

$$\rho_r = (P_r + E_m)^{D_m} / F_m \tag{5}$$

where $\rho_r = \rho/\rho_{cm}$ and $P_r = P/P_{cm}$. The subscript m denotes mixtures and the parameters D_m, E_m, and F_m are defined as follows:

$$D_m = d_1 + d_2\tau \tag{6}$$

$$E_m = e_1\tau + e_2\tau^2 + e_3\tau^4 \tag{7}$$

$$F_m = f_1 + f_2\tau + f_3\tau^2 + f_4\tau^4 \tag{8}$$

where $\tau = 1 - T/T_{cm}$.

We applied a simple mixing rule for each numerical constant as given in Eq. (9). The data used to determine the parameter values in Eq. (9) are the present saturated- and compressed-liquid densities and those of Widiatmo et al. [7]. The values of the numerical parameters are summarized in Table V.

$$Y_i = x_1 Y_{i,1} + (1 - x_1) Y_{i,2} + x_1(1 - x_1) Y_{i,12} \qquad (Y = d, e, f) \tag{9}$$

x_{125} denotes the mole fraction of R-125. The deviations of liquid densities from Eq. (5) are plotted in Figs. 5 and 6. As shown in Figs. 5 and 6, most of the present data and the data of Widiatmo et al. [7] agree with Eq. (5) within $\pm 0.2\%$. The effective range of Eq. (5) covers temperatures from 280 to 330 K and pressures up to 3 MPa.

Table V. Numerical Constants in Eq. (9)

d_i		e_i		f_i	
d_1		e_1		f_1	
$d_{1,1}$	0.42711	$e_{1,1}$	44.623	$f_{1,1}$	0.73408
$d_{1,2}$	0.51492	$e_{1,2}$	33.936	$f_{1,2}$	0.69840
$d_{1,12}$	0.088299	$e_{1,12}$	−0.019953	$f_{1,12}$	0.013143
d_2		e_2		f_2	
$d_{2,1}$	0.21891	$e_{2,1}$	331.42	$f_{2,1}$	5.6292
$d_{2,2}$	−0.0010140	$e_{2,2}$	317.66	$f_{2,2}$	6.4454
$d_{2,12}$	−0.058131	$e_{2,12}$	−0.098548	$f_{2,12}$	3.2364
		e_3		f_3	
		$e_{3,1}$	−0.94528	$f_{3,1}$	−0.095887
		$e_{3,2}$	2050.3	$f_{3,2}$	3.3030
		$e_{3,12}$	−0.00012525	$f_{3,12}$	−1.0378
				f_4	
				$f_{4,1}$	13.109
				$f_{4,2}$	13.206
				$f_{4,12}$	−0.24057

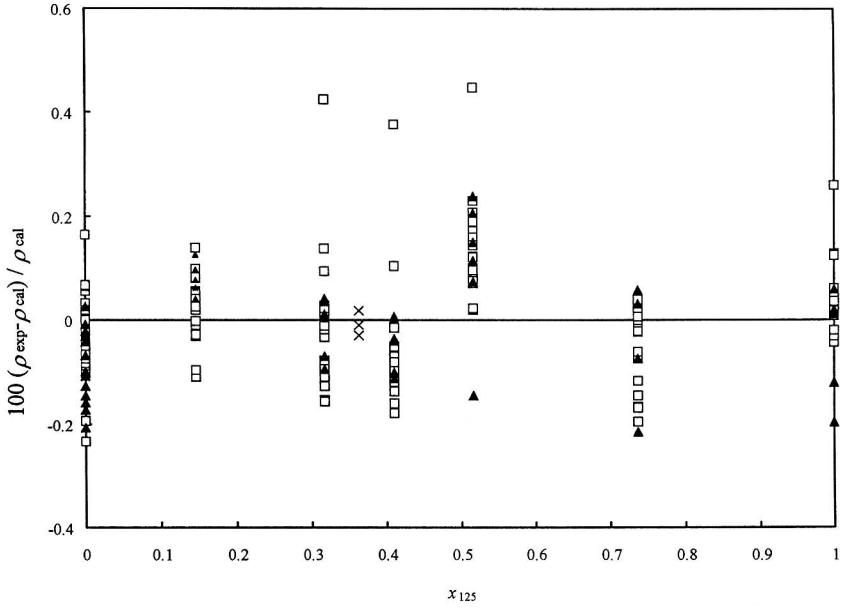

Fig. 5. Relative deviations of liquid densities at different compositions from Eq. (5). This work: ▲, saturated-liquid densities; □, compressed-liquid densities. ×, Widiatmo et al. [7].

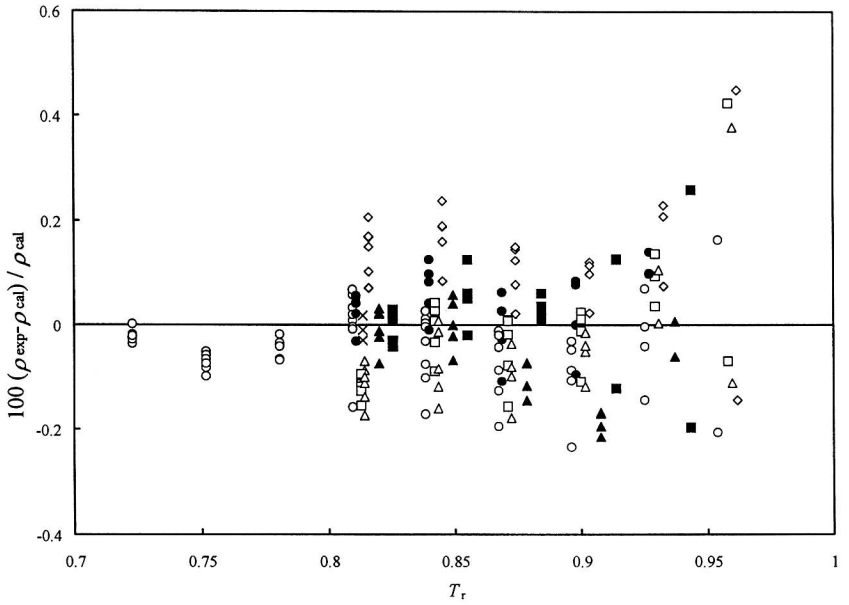

Fig. 6. Relative deviations of liquid densities at different temperatures from Eq. (5). This work: ○, 0 mass% R-125; ●, 20 mass% R-125; □, 40 mass% R-125; △, 50 mass% R-125; ◇, 60 mass% R-125; ▲, 80 mass% R-125; ■, 100 mass% R-125. ×, Widiatmo et al. [7].

4. CONCLUSIONS

One-hundred sixty-eight compressed-liquid $P\rho Tx$ state points, including essential thermodynamic properties at the two-phase condition of the binary R-125 + R-143a system, were measured over a range of temperatures from 280 to 330 K and pressures up to 3 MPa at compositions of 0, 19.64, 39.98, 49.91, 60.39, 80.00, and 100 mass% R-125.

The optimized PR equation can reproduce most of the available bubble-point pressure data within $\pm 2\%$. The saturated-liquid densities are also well represented within $\pm 0.3\%$ by the correlation for saturated-liquid density. The compressed-liquid $P\rho Tx$ properties are satisfactorily represented by the equation of state within $\pm 0.2\%$ in density.

ACKNOWLEDGMENTS

We are indebted to Asahi Glass Co. Ltd., Tokyo, and Daikin Industries, Ltd., Osaka, for their valuable cooperation in furnishing the research-grade samples of R-125 and R-143a. The assistance of Akina Kozakai is also greatly acknowledged.

REFERENCES

1. J. V. Widiatmo, H. Sato, and K. Watanabe, *Fluid Phase Equil.* **99**:199 (1994).
2. J. V. Widiatmo, H. Sato, and K. Watanabe, *Proc. Asia-Pacific Conf. Built Environ.* (1995), p. 253.
3. J. V. Widiatmo, H. Sato, and K. Watanabe, *J. Chem. Eng. Data* **42**:270 (1997).
4. International Organization for Standardization, *Guide to the Expression of Uncertainty in Measurement* (Switzerland, 1993).
5. M. Nagel and K. Bier, *Int. J. Refrig.* **18**:264 (1995).
6. Y. Higashi, *Proc. 1996 JAR Annu. Conf.* (1996), p. 93 (in Japanese).
7. J. V. Widiatmo, H. Sato, and K. Watanabe, *Int. J. Thermophys.* **16**:801 (1995).
8. J. V. Widiatmo, H. Sato, and K. Watanabe, *Proc. 16th Japan Symp. Thermophys. Prop.* (1995), p. 181.
9. T. Ikeda and Y. Higashi, *Proc. 16th Japan Symp. Thermophys. Prop.* (1995), p. 169 (in Japanese).
10. H. Sato, Ph.D. dissertation (Keio University, Yokohama, Japan, 1981) (in Japanese).
11. H. Takashima and Y. Higashi, *Proc. 16th Japan Symp. Thermophys. Prop.* (1995), p. 9 (in Japanese).
12. V. Zhelezny, Y. Chernyak, V. Anisomov, Y. Semenyuk, and P. Zhelezny, *Proc. 4th Asian Thermophys. Prop. Conf., Tokyo, Japan* (1995), p. 335.
13. G. Kishizawa, H. Sato, and K. Watanabe, *Int. J. Thermophys.* **20**:923 (1999).